Portable optical tissue flow oximeter based on diffuse correlation spectroscopy

Yu Shang,[1] Youquan Zhao,[1,2] Ran Cheng,[1] Lixin Dong,[1] Daniel Irwin,[1] and Guoqiang Yu[1,*]

[1]*Center for Biomedical Engineering, University of Kentucky, Lexington, Kentucky 40506, USA*
[2]*Department of Biomedical Engineering, Tianjin University, Tianjin 300072, China*
**Corresponding author: guoqiang.yu@uky.edu*

Received June 19, 2009; revised September 8, 2009; accepted October 7, 2009;
posted October 21, 2009 (Doc. ID 113026); published November 12, 2009

A portable diffuse correlation spectroscopy (DCS) *flowmeter* has been extended to measure both tissue blood flow and oxygenation (namely, DCS *flow oximeter*). For validation purposes, calf muscle blood oxygenation during cuff inflation and deflation was measured concurrently using the DCS flow oximeter and a commercial tissue oximeter. The oxygenation traces from the two measurements exhibited similar dynamic responses, and data were highly correlated ($r_{mean}>0.9$, $P<10^{-5}$, $n=10$). The portable, inexpensive, and easy-to-use DCS flow oximeter holds promise for bedside monitoring of tissue blood flow and oxygenation in clinics.

OCIS codes: 170.0170, 170.3660, 170.3880, 170.6480.

A wide range of noninvasive techniques exists for the study of deep tissue hemodynamics including magnetic resonance imaging (MRI), positron emission tomography, single photon emission computed tomography, and xenon computed tomography. However, the routine use of these techniques in clinics is limited owing to the availability, the expense, and the difficulty of making continuous measurements at the bedside. As an exciting alternative, near-IR (NIR) light has been shown to penetrate into deep tissues (up to several centimeters) for the measurement of regional tissue oxygenation [1–4]. A novel technology, the NIR diffuse correlation spectroscopy (DCS) flowmeter, has recently been developed for the noninvasive measurement of the relative change of blood flow (rBF) in deep tissues [5–10]. Measurements of rBF by the DCS flowmeter have been validated against Doppler ultrasound [8], laser Doppler [5], and perfusion MRI [9]. The technology has also been combined with an NIR diffuse reflectance spectroscope (DRS) tissue oximeter to form a hybrid instrument [5,10]. This allows for the simultaneous measurements of tissue blood flow and oxygenation, thus directly probing the tissue oxygen metabolism [10].

The existing hybrid instrument (DCS+DRS) is large, complex, and expensive. Thus we sought to build and validate a portable, easy-to-use, and inexpensive optical device for bedside monitoring of deep tissue hemodynamics. For this purpose, we added a second laser diode to the portable DCS flowmeter and measured light intensities at two wavelengths (785 and 854 nm) to extract tissue oxygenation information. We name this device the "DCS flow oximeter" as it measures both blood flow and oxygenation.

DCS uses the NIR light to detect the motion of red blood cells in tissues [5–10]. The DCS flow oximeter, shown in Fig. 1(a), consists of a cw laser diode (785 nm, 100 mW, Crystalaser, Inc.) with a long coherence length (>5 m), four single-photon-counting avalanche photodiodes (APDs, Pacer, Inc.), and a four-channel correlator (Correlator.com). Photons are emitted from the laser source, travel through the tissue, and are scattered back to the detectors. The detector signals are fed into the correlator yielding four autocorrelation curves every 44 ms. In this study, multiple correlation curves were averaged within ~1.2 s to get one flow value with an adequate signal-to-noise ratio. Blood flow information is extracted by fitting the averaged/smoothed autocorrelation curve whose decay rate depends mainly on the motion of red blood cells [5–10].

To measure tissue oxygenation, a second cw laser diode (854 nm, 120 mW) with a long coherence length and a transistor-transistor logic control unit, alternately switching between the two wavelengths, were added to the DCS device [see Fig. 1(a)]. Notice that the wavelengths were chosen based on the lasers available. Optimization of wavelengths [3] will be the subject of future work. The oxygenation information was extracted by recording the average detected light intensities at two wavelengths ($\lambda_1=785$ nm and $\lambda_2=854$ nm). The changes in oxyhemoglobin and deoxyhemoglobin concentrations ($\Delta[HbO_2]$ and $\Delta[Hb]$, respectively) relative to their baseline values (determined before physiological changes) were calculated based on the modified Beer–Lambert law [3],

$$\Delta[HbO_2]=\frac{\varepsilon_{Hb}(\lambda_1)\Delta\mu_a(\lambda_2)-\varepsilon_{Hb}(\lambda_2)\Delta\mu_a(\lambda_1)}{\varepsilon_{Hb}(\lambda_1)\varepsilon_{HbO_2}(\lambda_2)-\varepsilon_{HbO_2}(\lambda_1)\varepsilon_{Hb}(\lambda_2)},$$

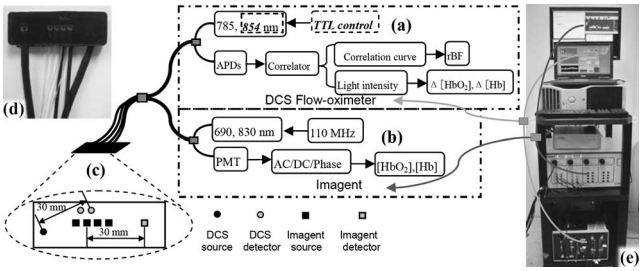

Fig. 1. Hybrid system combining the DCS flow oximeter and Imagent: (a) DCS flow oximeter, (b) Imagent, (c) hybrid probe, (d) probe photograph, (e) hybrid system photograph.

$$\Delta[\mathrm{Hb}] = \frac{\varepsilon_{\mathrm{HbO}_2}(\lambda_2)\Delta\mu_a(\lambda_1) - \varepsilon_{\mathrm{HbO}_2}(\lambda_1)\Delta\mu_a(\lambda_2)}{\varepsilon_{\mathrm{Hb}}(\lambda_1)\varepsilon_{\mathrm{HbO}_2}(\lambda_2) - \varepsilon_{\mathrm{HbO}_2}(\lambda_1)\varepsilon_{\mathrm{Hb}}(\lambda_2)}. \quad (1)$$

Here $\Delta\mu_a(\lambda) = \ln(I_{\lambda B}/I_{\lambda T})/(d\ \mathrm{DPF}_\lambda)$ [1], where $\Delta\mu_a(\lambda)$ is the relative change in the tissue absorption coefficient at wavelength λ. $\varepsilon_{\mathrm{HbO}_2}(\lambda)$ and $\varepsilon_{\mathrm{Hb}}(\lambda)$ are the extinction coefficients of oxyhemoglobin and deoxyhemoglobin. $I_{\lambda B}$ and $I_{\lambda T}$ are the measured light intensities at the baseline and at time T, respectively. The differential path length factor (DPF_λ) denotes the ratio of the mean photon path length to the distance (d) between the source and the detector pair. The DPF depends primarily on the tissue optical properties (i.e., reduced scattering coefficient μ_s' and μ_a) measured by frequency-domain (FD) or time-domain systems [1,4]. However, most studies using cw systems assume a constant DPF (from the literature), which could potentially influence the evaluation of $\Delta[\mathrm{Hb}]$ and $\Delta[\mathrm{HbO}_2]$. In this study, we compare the calculation results in $\Delta[\mathrm{Hb}]$ and $\Delta[\mathrm{HbO}_2]$ using three different DPFs: (1) "continuous DPF," calculated at each time point by a commercial FD tissue oximeter, the Imagent (Iss, Inc.) [11,12]; (2) "baseline DPF," obtained by averaging the baseline continuous DPFs; and (3) "literature DPF," assumed based on [4].

For validation purposes, we conducted concurrent measurements of skeletal muscle oxygenation using the Imagent and the DCS flow oximeter. The Imagent shown in Fig. 1(b) is an FD instrument, which consists of a photomultiplier tube (PMT) and eight laser diodes (four at 690 nm and four at 830 nm) modulated at 110 MHz. Multiple laser diodes time share the PMT. A heterodyne detection circuit is used to detect amplitudes (ac and dc) and phases of the reflected light for the extraction of absolute μ_a, μ_s', [Hb], and [HbO_2] [11,12]. The Imagent was selected for comparison/validation since the heterodyne detection system provides a higher signal-to-noise ratio than the homodyne DRS detection system we have used previously. The Imagent has been successfully used by many groups for tissue oxygenation measurements [11,12].

A hybrid fiber-optic probe [see Figs. 1(c) and 1(d)] was constructed, which covered approximately the same volume of tissue for both devices. Based on our testing results, the sources of the DCS flow oximeter/Imagent were arranged 54 mm/7 mm away from the Imagent/DCS detectors to avoid damaging the very sensitive PMT/APDs. All the fibers were held by a soft foam pad and aligned to cover the middle region of the probe. The source–detector separations used were 2.5 and 3.0 cm for the DCS flow oximeter and 2.0, 2.5, 3.0, and 3.5 cm for the Imagent. Multiple separation measurements provide information about tissue heterogeneous responses at different regions and depths [10]. In this study, the data obtained from the larger separation (3.0 cm) were used to compare the hemodynamic responses measured by the two devices since more overlapped region was covered by the larger separation pairs (see Fig. 1), thus reducing the influence of tissue heterogeneous responses. Moreover, amplitudes and phases at multiple separations were used to extract absolute values of μ_a and μ_s' for the calculation of the DPF [1]. The two devices worked sequentially using trigger signals controlled by custom software [see Fig. 1(e)]. In total, the data acquisition time was 3.0 s (2.4 s for the two DCS wavelengths and 0.6 s for averaging the Imagent data).

With Institutional Review Board approval consents, ten healthy volunteers lay supine and a cuff-occlusion paradigm was used to manipulate skeletal muscle hemodynamics. The optical probe was taped on the calf flexor and a cuff tourniquet was placed on the thigh to generate occlusion. The experimental protocol consists of repeating the following sequence twice: 2 min baseline, 5 min cuff inflation (250 mmHg), and 5 min recovery following the deflation.

Figure 2 shows the typical calf rBF from one subject during the occlusion. The two flow curves exhibited highly consistent dynamics. This consistency was observed in each of the remaining subjects, indicating that DCS flow signals from muscles are insensitive to wavelength. On average ($n=10$), the peak rBF following the cuff deflation was (357.3±142.9)% for 785 nm and (350.7±159.9)% for 854 nm compared with their baselines (assigned 100%), while their respective time-to-peaks were 49.2±13.5 and 49.5±13.2 s. These results are in agreement with our previous measurements using a DCS flowmeter at one wavelength [9,10].

Figure 3 shows the typical dynamic changes in [HbO_2] and [Hb] measured from the same volunteer. The oxygenation traces from the two measurements exhibited similar dynamic responses. Significant linear correlations in $\Delta[\mathrm{HbO}_2]$ ($r=0.96$, $P<10^{-5}$) and $\Delta[\mathrm{Hb}]$ ($r=0.97$, $P<10^{-5}$) were observed (see Fig. 4).

Significant correlations between the two measurements were found from all of the ten subjects. Figure 5 shows the means and the standard deviations of the correlation coefficients (r) in $\Delta[\mathrm{HbO}_2]$ and $\Delta[\mathrm{Hb}]$ for the two repeated tests. These correlations were excellent ($r_{\mathrm{mean}}>0.9$, $P<10^{-5}$, $n=10$) and not significantly affected by using different DPF values. The maximal differences in correlation coefficients between the two repeated tests are also small ((4.4±3.9)% for $\Delta[\mathrm{HbO}_2]$ and (1.4±1.2)% for $\Delta[\mathrm{Hb}]$).

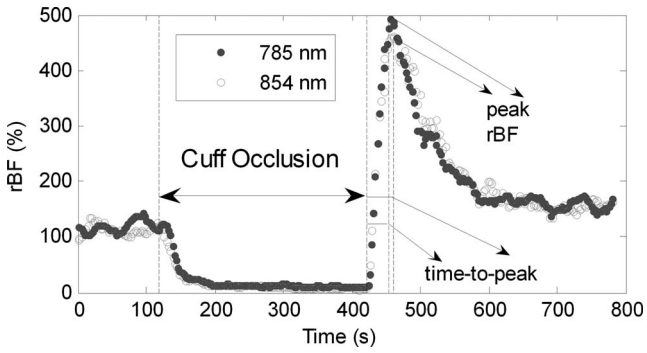

Fig. 2. Typical rBF responses in calf muscle during occlusion measured by the DCS flow oximeter at two wavelengths (785 and 854 nm). Blood flow responses were characterized by peak rBF (%) and time-to-peak (s).

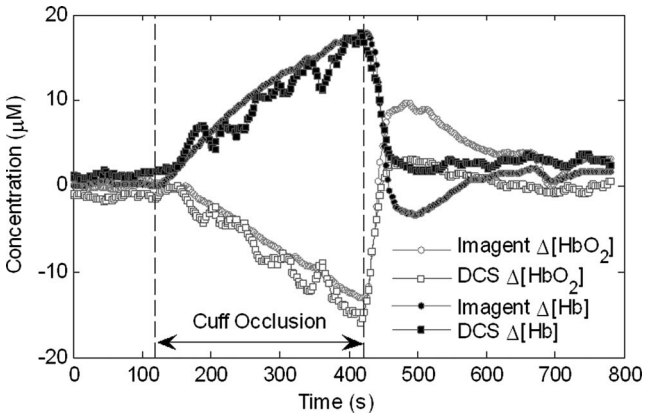

Fig. 3. Typical calf muscle responses in $\Delta[HbO_2]$ and $\Delta[Hb]$ during occlusion measured by the Imagent and DCS flow oximeter. Oxygenation data were calculated using the continuous DPF.

The slopes of regression lines (see typical examples in Fig. 4) for the first test ($n=10$) are 0.78 ± 0.31, 0.77 ± 0.32, and 0.79 ± 0.34 for $\Delta[HbO_2]$ and 0.94 ± 0.29, 0.91 ± 0.31, and 0.95 ± 0.36 for $\Delta[Hb]$, corresponding to the respective three DPF values. The small measurement discrepancies (slopes are not equal to 1) may be due to the instrumentation differences in wavelengths used, the methods (FD versus cw), the mismatch of tissue volumes probed, and the time delay in obtaining data at different wavelengths of sources. Such discrepancies between different tissue oximeters have been reported elsewhere [2]. Further device calibrations are being conducted using tissue phantoms.

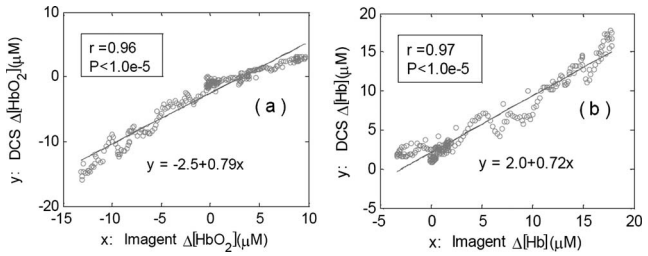

Fig. 4. Correlations between the Imagent and DCS flow-oximeter measurements in (a) $\Delta[HbO_2]$ and (b) $\Delta[Hb]$.

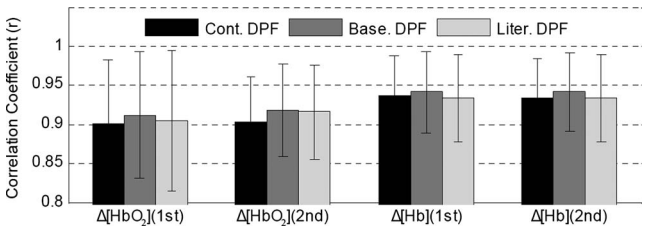

Fig. 5. Correlations between the Imagent and DCS flow-oximeter measurements in two repeated tests (first versus second). Oxygenation data were calculated using continuous, baseline, and literature DPFs, respectively.

This Letter reports a portable DCS-based flow oximeter that can simultaneously measure the rBFs and oxygenation in deep tissues. This device employs what we believe to be a new design with significantly less cost (1/2), smaller size (1/5), simpler construction, and easier operation compared with the existing hybrid instrument (DCS+DRS). The new probe shares source and detector fibers for both flow and oxygenation measurements, thus covering exactly the same tissue volume. This avoids any measurement discrepancies owing to tissue heterogeneity. The oxygenation measurements have been validated against a commercial tissue oximeter (Imagent), while the blood flow dynamics are consistent with our published results. The portable design of the DCS flow oximeter makes it possible to be used at the bedside of clinics (e.g., intensive care/therapy unit).

We acknowledge support from the American Heart Association (BGIA-0665446U and BGIA-2350015) and National Institutes of Health (NIH) (HL-083225).

References

1. S. Fantini, D. Hueber, M. A. Franceschini, E. Gratton, W. Rosenfeld, P. G. Stubblefield, D. Maulik, and M. R. Stankovic, Phys. Med. Biol. **44**, 1543 (1999).
2. R. E. Gagnon, A. J. Macnab, F. A. Gagnon, D. Blackstock, and J. G. LeBlanc, J. Clin. Monit. **17**, 385 (2002).
3. G. Strangman, M. A. Franceschini, and D. A. Boas, Neuroimage **18**, 865 (2003).
4. A. Duncan, J. H. Meek, M. Clemence, C. E. Elwell, L. Tyszczuk, M. Cope, and D. T. Delpy, Phys. Med. Biol. **40**, 295 (1995).
5. C. Cheung, J. P. Culver, K. Takahashi, J. H. Greenberg, and A. G. Yodh, Phys. Med. Biol. **46**, 2053 (2001).
6. L. Gagnon, M. Desjardins, J. Jehanne-Lacasse, L. Bherer, and F. Lesage, Opt. Express **16**, 15514 (2008).
7. J. Li, M. Ninck, L. Koban, T. Elbert, J. Kissler, and T. Gisler, Opt. Lett. **33**, 2233 (2008).
8. G. Yu, T. Durduran, C. Zhou, H. W. Wang, M. E. Putt, H. M. Saunders, C. M. Sehgal, E. Glatstein, A. G. Yodh, and T. M. Busch, Clin. Cancer Res. **11**, 3543 (2005).
9. G. Yu, T. F. Floyd, T. Durduran, C. Zhou, J. J. Wang, J. A. Detre, and A. G. Yodh, Opt. Express **15**, 1064 (2007).
10. G. Yu, T. Durduran, G. Lech, C. Zhou, B. Chance, E. R. Mohler, and A. G. Yodh, J. Biomed. Opt. **10**, 024027 (2005).
11. D. Choudhury, B. Michener, P. Fennelly, and M. Levi, J. Vasc. Technol. **23**, 21 (1999).
12. U. Wolf, M. Wolf, J. H. Choi, M. Levi, D. Choudhury, S. Hull, D. Coussirat, L. A. Paunescu, L. P. Safonova, A. Michalos, W. W. Mantulin, and E. Gratton, J. Vasc. Surg. **37**, 1017 (2003).